

# Discontinuous collocation and symmetric integration methods for distributionally-sourced hyperboloidal partial differential equations

Michael F. O'Boyle<sup>1,\*</sup> and Charalampos Markakis<sup>2,3</sup>

<sup>1</sup> Grainger College of Engineering, University of Illinois at Urbana-Champaign, Urbana, Illinois 61801, USA

<sup>2</sup> Mathematical Sciences, Queen Mary University of London, E1 4NS, London, UK

<sup>3</sup> NCSA, University of Illinois at Urbana-Champaign, Urbana, Illinois 61801, USA

---

**Abstract.** This work outlines a time-domain numerical integration technique for linear hyperbolic partial differential equations sourced by distributions (Dirac  $\delta$ -functions and their derivatives). Such problems arise when studying binary black hole systems in the extreme mass ratio limit. We demonstrate that such source terms may be converted to effective domain-wide sources when discretized, and we introduce a class of time-steppers that directly account for these discontinuities in time integration. Moreover, our time-steppers are constructed to respect time reversal symmetry, a property that has been connected to conservation of physical quantities like energy and momentum in numerical simulations. To illustrate the utility of our method, we numerically study a distributionally-sourced wave equation that shares many features with the equations governing linear perturbations to black holes sourced by a point mass.

**AMS subject classifications:** 35Q75, 65D30, 65M20, 65M22, 65M70, 83-10, 83C25

**Key words:** Symmetric integration, Hermite integration, discontinuous collocation methods, black hole perturbation theory, hyperboloidal slicing

---

## 1 Introduction

For radiation-reaction forces in electrodynamics and gravitational self-force corrections in general relativity [5, 56], the source of reduced field equations is distributional, leading to non-analyticity in the field at the particle's location. Previous solutions have ranged from multi-domain pseudospectral methods and discontinuous Galerkin methods with time-dependent mapping [15–17, 25, 26, 40, 42], to finite-difference methods based on null coordinates or representations of the Dirac  $\delta$  function [6–8, 35, 36, 38, 47, 48, 52, 60, 61]. The

---

\*Corresponding author. *Email address:* mboyle2@illinois.edu

former two methods employ a ‘‘Lagrangian’’ perspective in that the particle is treated with co-moving coordinates (albeit in a decomposed domain), while the latter three employ an ‘‘Eulerian’’ perspective in that the particle moves with respect to fixed coordinates. The methods proposed here leverage the advantages of both perspectives, integrating high order derivative jumps for finite-difference or pseudospectral implementations in Eulerian coordinates without domain decomposition.

Existing methods for handling non-analyticities often incur significant computational cost and complexity, or sacrifice accuracy [10]. Post-processing of oscillatory data can recover spectrally convergent non-oscillatory solutions, but these techniques can also be computationally expensive and prone to complications [2–4, 11, 28–34, 43, 55, 59].

Existing methods for approximating piecewise smooth functions, such as those introduced by Krylov [44], Lanczos [45] and Eckhoff [20–24, 53], or those that use polynomial correction terms as in Lipman and Levin [46], often scale poorly or face other complications. In contrast, Lipman and Levin’s method, uses moving least squares to determine the location and magnitude of a discontinuity, and its computational cost scales more favorably, comparable to  $O(N)$  rather than  $O(N^2)$ .

Explicit time-evolution schemes, such as classical Runge-Kutta methods, are prevalent in numerical relativity, despite their drawbacks: conditional stability (CFL limitation) and energy/symplectic structure violations in Hamiltonian systems. This ambiguity in energy loss cause can pose issues in gravitational wave (GW) computations. An alternative is a *geometric integrator*, which upholds key aspects of Hamiltonian dynamics, like symplecticity or time-reversal symmetry [37, 58]. While no method can universally preserve both energy and symplectic structure in a Hamiltonian system, this can be possible for quadratic Hamiltonians [14, 19, 66], such as those arising in black hole perturbation theory.

Integrators which respect time-reversal symmetry are especially appealing to physics problems because they have been shown to have intimate connections to conservation in numerical dynamics [50, 51, 54]. In addition, these schemes are implicit, which endows them with unconditional stability [12, 13]. By removing the CFL limit, these methods allow larger timesteps, overcome numerical instability, and speed up evolutions, making them suitable for long-time simulations of events like LISA band GWs.

In what follows, we consider distributionally-sourced partial differential equations (PDEs) of the 1+1 form

$$\square\Psi_{\ell m} = F_{\ell m}(t, x) \delta'(x - \zeta(t)) + G_{\ell m}(t, x) \delta(x - \zeta(t)) \quad (1.1)$$

where  $\square$  is a generalized d’Alembert operator in a curvilinear coordinate chart  $\{t, x\}$  and  $x = \zeta(t)$  is the worldline of a point particle in this chart. Here, we assume that the field  $\Psi_{\ell m}$  has been expanded in spherical harmonic modes  $\ell, m$  so that the remaining d’Alembert operator is 1+1. The main difficulty is that  $\Psi_{\ell m}$  and its time or space derivatives are discontinuous across the particle’s worldline. The methods discussed here exploit the fact that the location and magnitude of these jump discontinuities can be determined in advance, in terms of  $F_{\ell m}, G_{\ell m}$  and  $\zeta(t)$ . Below, for completeness, we summarize earlier work on discontinuous collocation methods [50] for solving equations of the above form.

We then extend our discontinuous time-symmetric integration formulae from second to fourth order. We demonstrate the utility of these schemes in the case of a wave equation sourced by a moving particle on hyperboloidal slices of Minkowski spacetime. Throughout this work, we adopt so-called geometric units where  $c = 1$  and time coordinates have the same units as space coordinates.

## 2 Discontinuous collocation methods

Here, for completeness, we outline the derivation of discontinuous collocation methods (cf. [46, 50, 54] for original details) which are used in §4 to solve distributionally-sourced PDEs. The methods of §2 are designed to model discontinuities in space, which suffices for static sources. For moving sources, one must also model discontinuities in time, as discussed in §3.

### 2.1 Piecewise smooth interpolation

Let  $f: [a, b] \rightarrow \mathbb{R}$  be a  $C^k$  function, with the values  $f_i = f(x_i)$  known at the ordered, distinct nodes  $x_i$  ( $a \leq x_0 < x_1 < \dots < x_N \leq b$ ). Interpolation with a Lagrange polynomial of degree  $N$  is limited by the degree of differentiability, that is,  $N+1 \leq k$ . A degree of differentiability  $k$  lower than  $N+1$  necessitates modification of standard Lagrange interpolation. If  $f$  is a piecewise- $C^{N+1}$  function and its jump discontinuities are known, then a simple generalization of the Lagrange method to any  $k \geq -1$  can be found.

Let the discontinuity be located at some  $\xi \in (a, b)$  and the jumps in  $f$  and its derivatives be given by:

$$f^{(m)}(\xi^+) - f^{(m)}(\xi^-) := J_m < \infty, \quad m = 0, 1, \dots, \infty, \quad (2.1)$$

where  $\xi^-$  and  $\xi^+$  denote the limits to  $\xi$  from below and above respectively. Approximate  $f$  by a piecewise polynomial that interpolates the given  $N+1$  nodes and has the above specified derivative jumps at the discontinuity:

$$p(x) = \theta(x - \xi)p_+(x) + \theta(\xi - x)p_-(x) \quad (2.2)$$

where

$$\theta(x) = \begin{cases} 1, & x > 0 \\ 1/2, & x = 0 \\ 0, & x < 0 \end{cases} \quad (2.3)$$

is the Heaviside step function, and

$$p_-(x) = \sum_{j=0}^N c_j^-(\xi) x^j, \quad p_+(x) = \sum_{j=0}^N c_j^+(\xi) x^j \quad (2.4)$$

denote the left and right interpolating polynomials. The polynomials  $p_-, p_+$  and the piecewise polynomial  $p$  depend on the location and magnitude of the discontinuity. To

determine  $c_j^\pm$  we use the method of undetermined coefficients. Given the ansatz (2.2), the collocation conditions become:

$$p(x_i) = f_i \iff \begin{cases} p_+(x_i) = f_i, & x_i > \xi \\ p_-(x_i) = f_i, & x_i < \xi \end{cases}. \quad (2.5)$$

The above  $N+1$  collocation conditions only determine half of the  $(2N+2)$  polynomial coefficients  $c_j^\pm$ . To close the system and determine the other half, one can impose the first  $N+1$  of the jump conditions (2.1). However, as higher order jumps may be more complicated, or harder to compute, or may introduce Runge-type oscillations (*cf.* [50]), we allow the number of jumps enforced to be a specifiable parameter. If we drop jumps in derivatives higher than order  $M \in [-1, N]$ , then the remaining coefficients are determined by the  $N+1$  jump conditions

$$p^{(m)}(\xi^+) - p^{(m)}(\xi^-) = p_+^{(m)}(\xi) - p_-^{(m)}(\xi) = \begin{cases} J_m, & m = 0, 1, \dots, M \\ 0, & m = M+1, \dots, N \end{cases}. \quad (2.6)$$

Lagrange interpolation is recovered when  $M = -1$  or  $J_m = 0$ .

The ansatz (2.4) does not amount to domain decomposition as it does not consist of two independent interpolating polynomials of order  $n$  and  $N-n$  matched at the discontinuity. Our ansatz covers a single domain  $[a, b]$  with a single piecewise polynomial of order  $N$  which has piecewise constant coefficients with a known jump at the discontinuity  $\xi$ .

Substituting Eq. (2.4) into the collocation conditions (2.5) and jump conditions (2.6) determines the coefficients  $c_j^\pm$ . Their explicit form is provided in Ref. [50]. However, it is more convenient to use a Lagrange basis, whence the piecewise polynomial interpolant reads:

$$p(x) = \sum_{j=0}^N [f_j + \Delta(x_j - \xi; x - \xi)] \pi_j(x), \quad (2.7)$$

where

$$\pi_j(x) = \prod_{\substack{k=0 \\ k \neq j}}^N \frac{x - x_k}{x_j - x_k} \quad (2.8)$$

are the Lagrange basis polynomials. The basis polynomials satisfy the standard conditions  $\pi_j(x_i) = \delta_{ij}$ , with  $\delta_{ij}$  denoting the Kronecker symbol, so that  $p(x)$  satisfies the collocation and jump conditions by construction. The piecewise polynomial interpolant depends on the location  $\xi$  of the discontinuity through the 2-point functions

$$\Delta(x_j - \xi; x - \xi) = [\theta(x - \xi)\theta(\xi - x_j) - \theta(\xi - x)\theta(x_j - \xi)] \kappa(x_j - \xi) \quad (2.9)$$

where

$$\kappa(x_j - \xi) := \sum_{m=0}^M \frac{J_m}{m!} (x_j - \xi)^m \quad (2.10)$$

are weights computed from the jump conditions at the discontinuity  $\xi$  given the nodes  $x_j$ . As expected, Lagrange interpolation is recovered when no jumps are present,  $K_m = 0$ .

Generally, the nodes and differentiation matrices can be computed and stored in memory. However, in the context of time-dependent partial differential equations with distributional sources, the location and magnitude of the discontinuity will generally change in every time step as the particle moves. Thus, it will be important to be able to evaluate Eqs. (2.9) and (2.10) efficiently. As Eq. (2.10) is polynomial in  $\delta\tilde{\xi}_j = x_j - \xi$ , it can be computed with higher computational efficiency and numerical precision in Horner form:

$$\kappa(\delta\tilde{\xi}) = J_0 + \delta\tilde{\xi} \left( J_1 + \delta\tilde{\xi} \left( \frac{J_2}{2!} + \delta\tilde{\xi} \left( \dots + \delta\tilde{\xi} \left( \frac{J_{M-1}}{(M-1)!} + \delta\tilde{\xi} \frac{J_M}{M!} \right) \dots \right) \right) \right). \quad (2.11)$$

This operation is vectorized and parallelized across all available cores for all components  $\delta\tilde{\xi}_i$  of  $\delta\tilde{\xi}$ . When evaluated on a node  $x = x_i$ , Eq. (2.9) simplifies to

$$\Delta(x_j - \xi; x_i - \xi) = [\theta(x_i - \xi) - \theta(x_j - \xi)] \kappa(x_j - \xi). \quad (2.12)$$

Since the prefactor in  $\Delta(x_j - \xi; x_i - \xi)$  is antisymmetric in  $i, j$  and  $\pi_j(x_i) = \delta_{ij}$  is symmetric, the correction  $\sum_j \Delta(x_j - \xi; x - \xi) \pi_j(x)$  in the interpolation formula (2.7) vanishes at each node  $x = x_i$ . This ensures that the collocation conditions (2.5) are satisfied.

## 2.2 Discontinuous differentiation

Differentiating the piecewise polynomial (2.7) yields finite-difference or pseudospectral approximations to the  $n$ -th derivative of  $f(x)$ . Evaluated at a node  $x = x_i$ , this yields

$$f^{(n)}(x_i) \simeq p^{(n)}(x_i) = \sum_{j=0}^N D_{ij}^{(n)} [f_j + \Delta(x_j - \xi; x_i - \xi)], \quad (2.13)$$

with the differentiation matrices  $D_{ij}^{(n)}$  given by

$$D_{ij}^{(n)} = \pi_j^{(n)}(x_i) = \left. \frac{d^n \pi_j(x)}{dx^n} \right|_{x=x_i} \quad (2.14)$$

It has been shown [50] that at least  $M^{\text{th}}$ -order convergence can be attained when the 2-point  $\Delta$  functions (2.12) are included in Eq. (2.13).

As mentioned above, for time-domain problems, as the discontinuity at  $\xi$  moves, one must efficiently update these correction terms in each time-step. Substituting Eq. (2.12) into (2.13) yields the expression

$$f^{(n)}_i \simeq \sum_{j=0}^N D_{ij}^{(n)} (f_j + \kappa_j \theta_i - \kappa_j \theta_j), \quad (2.15)$$

where  $f_i = f(x_i)$ ,  $f_i^{(n)} = f^{(n)}(x_i)$ ,  $\theta_i = \theta(x_i - \xi)$  and  $\kappa_i = \kappa(x_i - \xi)$  are vectors formed from the values of the respective functions on the set of grid-points  $\{x_i\}$ . We remark that the above formulae are valid for both pseudospectral and finite-difference methods, *cf.* [50] for explicit expressions of the differentiation matrices.

On modern CPUs and GPUs, Eq. (2.15) can be evaluated efficiently via inner (dot product) matrix-vector multiplication and elementwise vector-vector multiplication (Hadamard product). For instance, in Wolfram Language, the simple command

```
fn = Dn.f + (Dn.k)*th - Dn.(k*th)
```

(with  $f$  and  $fn$  denoting  $f_i$  and  $f_i^{(n)}$ ,  $Dn$  denoting the  $n^{\text{th}}$  order differentiation matrix given by Eq. (2.14), and  $th$ ,  $k$  denoting the vectors  $\theta_i$ ,  $\kappa_i$  respectively) uses the INTEL MATH KERNEL LIBRARY to automatically perform the linear algebra operations in Eq. (2.15) in parallel, across all available cores. Similar commands can be used to accelerate the computation of these products on Nvidia GPUs using cuBLAS.

### 3 Discontinuous time-symmetric integration schemes

The methods outlined in the previous section enable us to account for the non-analytic behavior of the target function at a single point along the spatial axis. However, the function is also non-analytic when the point is approached along the temporal axis. This indicates that standard time-steppers (e.g. Runge-Kutta methods) cannot be readily applied to this problem, as they assume the target function to be smooth. Our discontinuous method-of-line experiments [50] indeed showed that using ordinary time-steppers with the (spatially) discontinuous collocation method described above works accurately if the particle is static or stationary (on a circular orbit), but precision is lost and the method fails to converge when the particle is moving in the  $x$  direction. This is in keeping with a key observation made by Harms et al. [39] that finite-difference representations of a Dirac- $\delta$  function (like discontinuous collocation methods) converge for a stationary discontinuity but not for a moving discontinuity. We will show here that the paradigm of using undetermined coefficients to accommodate known jump and collocation conditions can also be used to develop discontinuous time integration schemes. In §3.2 below we re-derive the second order discontinuous trapezium rule of [50] and in §3.3 we extend it to fourth order, obtaining a discontinuous generalization of the Hermite rule.

#### 3.1 Piecewise smooth time integration

For generality, we consider the first order differential equation

$$\frac{dy}{dt} = f(t, y) \quad (3.1)$$

on a small time interval  $[t_1, t_2]$ . This is equivalent to writing

$$y(t_2) - y(t_1) = \int_{t_1}^{t_2} f(t, y) dt, \quad (3.2)$$

so the problem is now to approximate the above integral. One approach is to construct a polynomial approximant to  $f$  between  $t_1$  and  $t_2$ . If the target function  $y(t)$  were smooth, it would be straightforward to construct a smooth approximant to  $f$  and integrate it to obtain a time-symmetric approximation to the integral, as shown in Ref. [51].

Now, though, we shall assume that  $y(t)$  is non-analytic at some point  $t_c \in (t_1, t_2)$  and that the discontinuities in  $f$  and all its derivatives at this point are known (which has been shown to be the case for linear distributionally-sourced PDEs [50]). Let  $K_n$  denote the discontinuity in the  $n^{\text{th}}$  time derivative of  $f$  at  $t = t_c$  when approached from from below. We accommodate this behavior by constructing the interpolant to be a *piecewise polynomial* of the form in Eq. (2.2), that is,

$$f(y, t) \simeq p(t) = \theta(t - t_c) p_+(t) + \theta(t_c - t) p_-(t). \quad (3.3)$$

Integrating the above interpolant yields discontinuous integration schemes. We provide second and fourth order symmetric integration schemes below.

### 3.2 Discontinuous trapezium rule

As discussed in Ref. [50]), the simplest interpolant which satisfies endpoint collocation conditions (e.g.  $f(t_1) = f_1$  and  $f(t_2) = f_2$ ) is a first order polynomial. It follows that the simplest interpolant that satisfies collocation conditions and the jump conditions  $K_n$  while preserving time symmetry is one that is first order to both the left and right of  $\tau$ . Such an interpolant has four parameters so

$$p_+(t) = A + Bt, \quad p_-(t) = C + Dt \quad (3.4)$$

Following the construction of the trapezium rule, we impose collocation at the endpoint, so  $p_-(t_1) = f_1$  and  $p_+(t_2) = f_2$ . We satisfy the remaining two degrees of freedom with jump conditions,  $p_+(t_c) - p_-(t_c) = K_0$ ,  $p'_+(t_c) - p'_-(t_c) = K_1$ . The resulting interpolant is

$$p_+(t) = f_1 \frac{t_2 - t}{\Delta t} + f_2 \frac{t - t_1}{\Delta t} + \frac{t_2 - t}{\Delta t} (K_0 - K_1(t_c - t_1)) \quad (3.5a)$$

$$p_-(t) = f_1 \frac{t_2 - t}{\Delta t} + f_2 \frac{t - t_1}{\Delta t} + \frac{t - t_1}{\Delta t} (-K_0 - K_1(t_2 - t_c)) \quad (3.5b)$$

Integrating the piecewise linear polynomial (3.3) over the time interval  $[t_1, t_2]$  yields a discontinuous generalization of the trapezium rule:

$$y_2 - y_1 \simeq \frac{\Delta t}{2} (f_1 + f_2) + K_0 \frac{\Delta t - 2\Delta t_c}{2} + K_1 \frac{\Delta t_c}{2} (\Delta t_c - \Delta t), \quad (3.6)$$

where  $\Delta t_c = \tau - t_1$ . We shall term this method DH2. The standard trapezium rule is obviously recovered when  $K_0 = K_1 = 0$ . Although we have not constructed an explicit remainder term, we find that, in practice, this expression exhibits second-order convergence in  $\Delta t$ .

### 3.3 Discontinuous Hermite rule

The next simplest interpolant that satisfies endpoint collocation is a third-order polynomial. It follows that the next simplest discontinuous piecewise interpolant should be cubic to both the left and right of  $\tau$ :

$$p_+(t) = A + Bt + Ct^2 + Dt^3, \quad p_-(t) = E + Ft + Gt^2 + Ht^3 \quad (3.7)$$

Following the same procedure as before, we impose the endpoint collocation conditions  $p_-(t_1) = f_1$ ,  $p_+(t_2) = f_2$ , osculation conditions  $p'_-(t_1) = f'_1$ ,  $p'_+(t_2) = f'_2$ , and jump conditions  $p_+(t_c) - p_-(t_c) = K_0$ ,  $p'_+(t_c) - p'_-(t_c) = K_1$ ,  $p''_+(t_c) - p''_-(t_c) = K_2$ , and  $p'''_+(t_c) - p'''_-(t_c) = K_3$ . The resulting interpolant is

$$\begin{aligned} p_+(t) = & \frac{(t_2-t)^2(2t+t_2-3t_1)}{\Delta t^3} f_1 - \frac{(2t+t_1-3t_2)(t-t_1)^2}{\Delta t^3} f_2 + \frac{(t_2-t)^2(t-t_1)}{\Delta t^2} f'_1 - \\ & \frac{(t_2-t)(t-t_1)^2}{\Delta t^2} f'_2 + \frac{(t_2-t)^2(2t-3t_1+t_2)}{\Delta t^3} K_0 \\ & - \frac{(t-t_2)^2(\Delta t_c(2t-3t_1+t_2) - (t-t_1)\Delta t)}{\Delta t^3} K_1 \\ & + \frac{(t_2-t)^2 \Delta t_c (\Delta t_c(2t-3t_1+t_2) - 2(t-t_1)\Delta t)}{2\Delta t^3} K_2 \\ & - \frac{\Delta t_c^2 (t_2-t)^2 (\Delta t_c(2t-3t_1+t_2) - 3(t-t_1)\Delta t)}{6\Delta t^3} K_3 \quad (3.8a) \end{aligned}$$

$$\begin{aligned} p_-(t) = & \frac{(t_2-t)^2(2t+t_2-3t_1)}{\Delta t^3} f_1 - \frac{(2t+t_1-3t_2)(t-t_1)^2}{\Delta t^3} f_2 + \frac{(t_2-t)^2(t-t_1)}{\Delta t^2} f'_1 \\ & - \frac{(t_2-t)(t-t_1)^2}{\Delta t^2} f'_2 + \frac{(t-t_1)^2(2t-3t_2+t_1)}{\Delta t^3} K_0 \\ & - \frac{(t-t_1)^2(\Delta t_c(2t-3t_2+t_1) + (2t_2-t-t_1)\Delta t)}{\Delta t^3} K_1 \\ & + \frac{(t-t_1)^2(t_2-\tau)(\Delta t_c(2t-3t_2+t_1) - 2\Delta t^2)}{2\Delta t^3} K_2 \\ & + \frac{(t-t_1)^2(t_2-\tau)^2(\Delta t_c(2t-3t_2+t_1) - (t-t_1)\Delta t)}{6\Delta t^3} K_3 \quad (3.8b) \end{aligned}$$

Integrating the piecewise cubic polynomial (3.3) over the interval  $[t_1, t_2]$  yields a discontinuous generalization of the Hermite rule:

$$\begin{aligned} y_2 - y_1 \simeq & \frac{\Delta t}{2} (f_1 + f_2) + \frac{\Delta t^2}{12} (f'_1 - f'_2) + K_0 \frac{\Delta t - 2\Delta t_c}{2} + K_1 \frac{\Delta t^2 - 6\Delta t \Delta t_c + 6\Delta t_c^2}{12} \\ & - K_2 \frac{\Delta t_c (\Delta t^2 - 3\Delta t \Delta t_c + 2\Delta t_c^2)}{12} + K_3 \frac{\Delta t_c^2 (\Delta t - \Delta t_c)^2}{24} \quad (3.9) \end{aligned}$$



We shall term this method DH4. The standard Hermite rule is recovered when the  $K_n$  are set to zero. As before, we find that, in practice, this expression exhibits fourth order convergence in  $\Delta t$  even though we have not computed a remainder.

### 3.4 Numerical experiment

We demonstrate the validity of these discontinuous integration schemes by studying how well they approximate the definite integral of a discontinuous function:

$$f(t) = P_5(t)\theta(t) + Q_3(t)\theta(-t) \quad (3.10)$$

where  $P_5$  is the fifth Legendre polynomial and  $Q_3$  is the third associated Legendre polynomial. The first four jumps, obviously located at  $t=0$ , may be calculated analytically:

$$K_0 = -\frac{2}{3}, \quad K_1 = \frac{15}{8}, \quad K_2 = 8, \quad K_3 = -\frac{105}{2} \quad (3.11)$$

We approximate the integral of this function over the interval  $[-0.51, 0.49]$  (this interval was chosen so that  $t=0$  is never located on a grid point, which Eqs. (3.6) and (3.9) implicitly assume), which may be calculated analytically to be  $\approx 0.294859$ .

In Figure 1, We observe that the approximation resulting from applying Eq. (3.6) to the subinterval containing  $t=0$  indeed exhibits error  $\mathcal{O}(\Delta t^2)$  and Eq. (3.9) exhibits error  $\mathcal{O}(\Delta t^4)$ , as we might expect from their construction. In addition, we note that the smooth versions of these expressions, without accounting for the jumps, result in poorly-behaved approximations.

## 4 Application to distributionally-sourced PDEs

### 4.1 Scalar wave equation with distributional source term

To illustrate the utility of both the discontinuous time stepping and spatial collocation schemes, we consider a simple prototype of a distributionally-sourced wave equation, and a variant of Eq. (1.1), considered previously in [25, 50]:

$$-\partial_t^2 \Psi + \partial_x^2 \Psi = F(t) \delta'(x - \zeta(t)) + G(t) \delta(x - \zeta(t)). \quad (4.1)$$

Heuristically, this equation gives the field produced by a scalar charge moving along the worldline  $\zeta(t)$  with a time-dependent monopole and dipole moment.

Eq. (4.1) possesses closed form solutions [25, 50] if the particle is taken to move at a constant speed  $v$  along a worldline  $\zeta(t) = vt$ . If  $F(t) = 0$  and  $G(t) = \cos t$ , "Solution I" is given by

$$\Psi_1(t, x) = -\frac{1}{2} \sin\left(\gamma^2(t - vx - |x - vt|)\right) \quad (4.2)$$

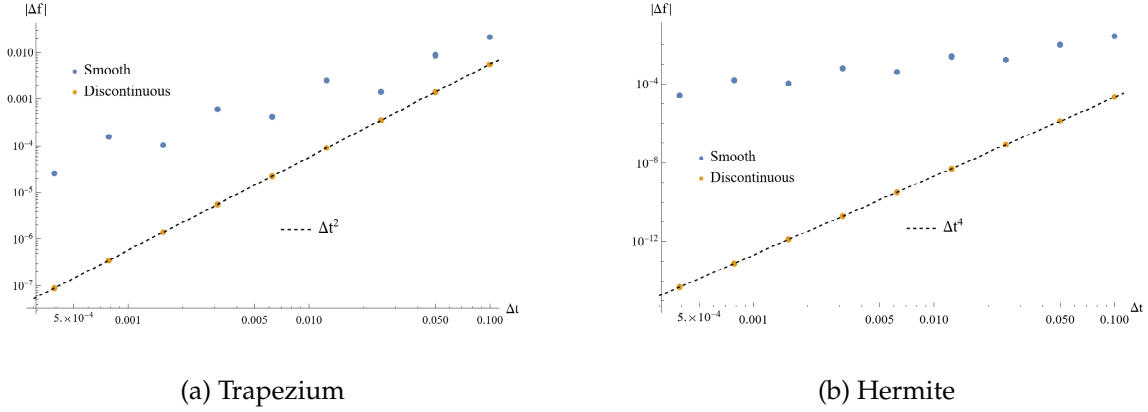


Figure 1: The error resulting from using Eqs. (3.6) (on the left) and (3.9) (on the right) to approximate the integral of Eq. (3.10) on the interval  $(-0.51, 0.49)$ . We observe that Eq. (3.6) exhibits second order convergence while Eq. (3.9) exhibits fourth order convergence while the smooth versions of these schemes result in poorly behaved approximations.

If  $F(t) = \sin t$  and  $G(t) = 0$ , “Solution II” is given by

$$\Psi_{\text{II}}(t, x) = \frac{1}{2} \gamma^2 (v + \text{sgn}(x - vt)) \cos(\gamma^2 (t - vx - |x - vt|)) \quad (4.3)$$

In prior work [50], the above solutions were used to test numerical solutions to Eq. (4.1) in Minkowski coordinates  $\{t, x\}$  using discontinuous time symmetric and discontinuous collocation methods. This required imposing boundary conditions at the ends of the spatial domain, which is generally not straightforward when a potential term is added to the above equation (as is necessary, for instance, in black hole perturbation theory). Here to automatically impose boundary conditions and improve computational efficiency, we adopt these numerical methods to hyperboloidal coordinates.

## 4.2 Hyperboloidal slicing

We adopt the method of *hyperboloidal compactification* developed by Zenginoglu [62–65]. As demonstrated in [49, 54], the idea is as follows. In Minkowski space, the null rays (characteristic curves of the scalar wave equation) form lines that are  $45^\circ$  from the  $t$ - and  $x$ -axes. If instead one defines a coordinate by

$$\tau = t - h(x) \quad (4.4)$$

and demands that

$$|h'(x)| < 1, \quad -\infty < x < \infty, \quad (4.5)$$

the new coordinate will be timelike throughout the interior of the domain. Moreover, if  $h$  satisfies

$$\lim_{x \rightarrow \pm\infty} h'(x) = \mp 1, \quad (4.6)$$

then the coordinate  $\tau$  will become null on the boundary surfaces and therefore intersect  $\mathcal{I}^+$ . Such a coordinate is termed *hyperboloidal*. Once this is achieved, one can bring the boundary surfaces into a finite domain via compactification; i.e. choose a new spacelike coordinate

$$x = g(\sigma) \quad (4.7)$$

such that

$$\sigma([-\infty, \infty]) = [0, 1] \quad (4.8)$$

Thus, such a set of coordinates maps the behaviors of the field on  $\mathcal{I}^+$  to finite spacelike and interior-timelike coordinates and preserves the initial value formulation for initial data given on a constant  $\tau$  slice  $\Sigma_\tau$ , making it ideal for numerical studies of GW generation.

Several such coordinate slicings have been found for the Minkowski, Schwarzschild and Kerr spacetime [27, 57, 65], but we find that the “minimal gauge” defined by Ansorg and Macedo [1] yields the simplest algebraic expressions and covers the entire black hole exterior with a single hyperboloidal layer. As written, the following compactification can be used in Minkowski as well as Schwarzschild spacetime (with  $t, x$  taken to be tortoise coordinates):

$$g(\sigma) := \int \frac{1}{2\sigma^2(\sigma-1)} = \frac{1}{2} \left( \frac{1}{\sigma} + \log(1-\sigma) - \log(\sigma) \right) \quad (4.9)$$

In [49], the asymptotic behavior of null rays was used to show that a suitable height function choice is:

$$h(\sigma) := g(\sigma) - \frac{1}{\sigma} + \ln\sigma + \mathcal{O}(\sigma). \quad (4.10)$$

Truncating this expression to linear order in  $\sigma$  amounts to the so-called “minimal gauge”. These expressions can be further generalized to Kerr spacetime [49].

Then, (4.1) can be written in the form

$$\begin{aligned} Z(\sigma)\partial_\tau^2\Psi + A(\sigma)\partial_\tau\partial_\sigma\Psi + B(\sigma)\partial_\tau\Psi + C(\sigma)\partial_\sigma^2\Psi + E(\sigma)\partial_\sigma\Psi \\ = F(\tau, \sigma)\delta'(\sigma - \zeta(\tau)) + G(\tau, \sigma)\delta(\sigma - \zeta(\tau)) \end{aligned} \quad (4.11)$$

Eq. (4.11) can be obtained from the 1+1 covariant wave equation,

$$\square_{\mathcal{N}^2}\Psi := \eta^{\alpha\beta}\nabla_\alpha\nabla_\beta\Psi = S, \quad (4.12)$$

on a flat manifold  $\mathcal{N}^2$  spanned by  $\tau$  and  $\sigma$ , where  $\eta_{\alpha\beta}$  is an effective Minkowski metric [41] given by the line element,

$$\eta_{\alpha\beta}dx^\alpha dx^\beta = -d\tau^2 + \frac{1-2\sigma^2}{\sigma^2(1-\sigma)} d\tau d\sigma + \frac{1+\sigma}{\sigma^2(1-\sigma)} d\sigma^2. \quad (4.13)$$

In the above coordinate chart, the wave operator for a scalar field is polynomial in  $\sigma$  and given by

$$\square_{\mathcal{N}^2}\Psi = -4\sigma^2(1-\sigma^2)\partial_\tau^2\Psi + 4\sigma^2(1-\sigma)(1-2\sigma^2)\partial_\tau\partial_\sigma\Psi + 4\sigma^4(1-\sigma)^2\partial_\sigma^2\Psi - 8\sigma^3(1-\sigma)\partial_\tau\Psi + 4\sigma^3(1-\sigma)(2-3\sigma)\partial_\sigma\Psi, \quad (4.14)$$

which allows the coefficients  $A, B, C, E$  and  $Z$  to be read off:

$$A(\sigma) = 1 - 2\sigma^2, \quad B(\sigma) = -2\sigma, \quad C(\sigma) = 1 - \sigma, \quad E(\sigma) = \sigma(2 - 3\sigma), \quad Z(\sigma) = 1 + \sigma. \quad (4.15)$$

To make manifest that outflow boundary conditions are automatically imposed at the boundaries  $\sigma = 0$  and  $\sigma = 1$  in this coordinate chart, we calculate the characteristic speeds of this wave equation,

$$v_+(\sigma) = \frac{\sigma^2}{1+\sigma}, \quad v_-(\sigma) = -1 + \sigma. \quad (4.16)$$

As required, the light cones tip over at the two boundaries, and we have  $v_+(0) = 0$  and  $v_-(1) = 0$ .

In the slicing of Eq. (4.13), the scalar solutions (4.2)-(4.3) of Eq. (4.1) transform to read

$$\Psi_{\text{I}}(\tau, \sigma) = \begin{cases} -\frac{1}{2} \sin\left(\frac{1+\sigma(\tau-\log\sigma)}{\sigma(1+v)}\right) & \sigma > \zeta(\tau) \\ -\frac{1}{2} \sin\left(\frac{\tau-\log(1-\sigma)}{1-v}\right) & \sigma < \zeta(\tau) \end{cases}, \quad (4.17)$$

$$\Psi_{\text{II}}(\tau, \sigma) = \begin{cases} -\frac{1}{2(1+v)} \cos\left(\frac{1+\sigma(\tau-\log\sigma)}{\sigma(1+v)}\right) & \sigma > \zeta(\tau) \\ \frac{1}{2(1-v)} \cos\left(\frac{\tau-\log(1-\sigma)}{1-v}\right) & \sigma < \zeta(\tau) \end{cases}, \quad (4.18)$$

where  $\zeta(\tau) = g^{-1}(\zeta(t))$  is the worldline of the particle in the hyperboloidal chart  $\{\tau, \sigma\}$ . This provides exact solutions by which to study the converge of our discontinuous time steppers below.

### 4.3 Generalized recursion relation

Before we turn the numerical evolution of specific problems, we first address the question of how jumps in the target function may be calculated in arbitrary coordinate systems. The method of unit jump functions presented in [50] may be extended to this situation, but it is significantly more involved than before.

Eq. (4.1) has been studied by Field et al. [25] and Markakis et al. [50]. Here, to develop the computational tools necessary for future hyperboloidal black hole perturbation applications, we study this equation on a hyperboloidal slice (4.13), given by Eq. (4.11). As in earlier work [50], we suppose that the general solution to Eq. (4.11) may be written

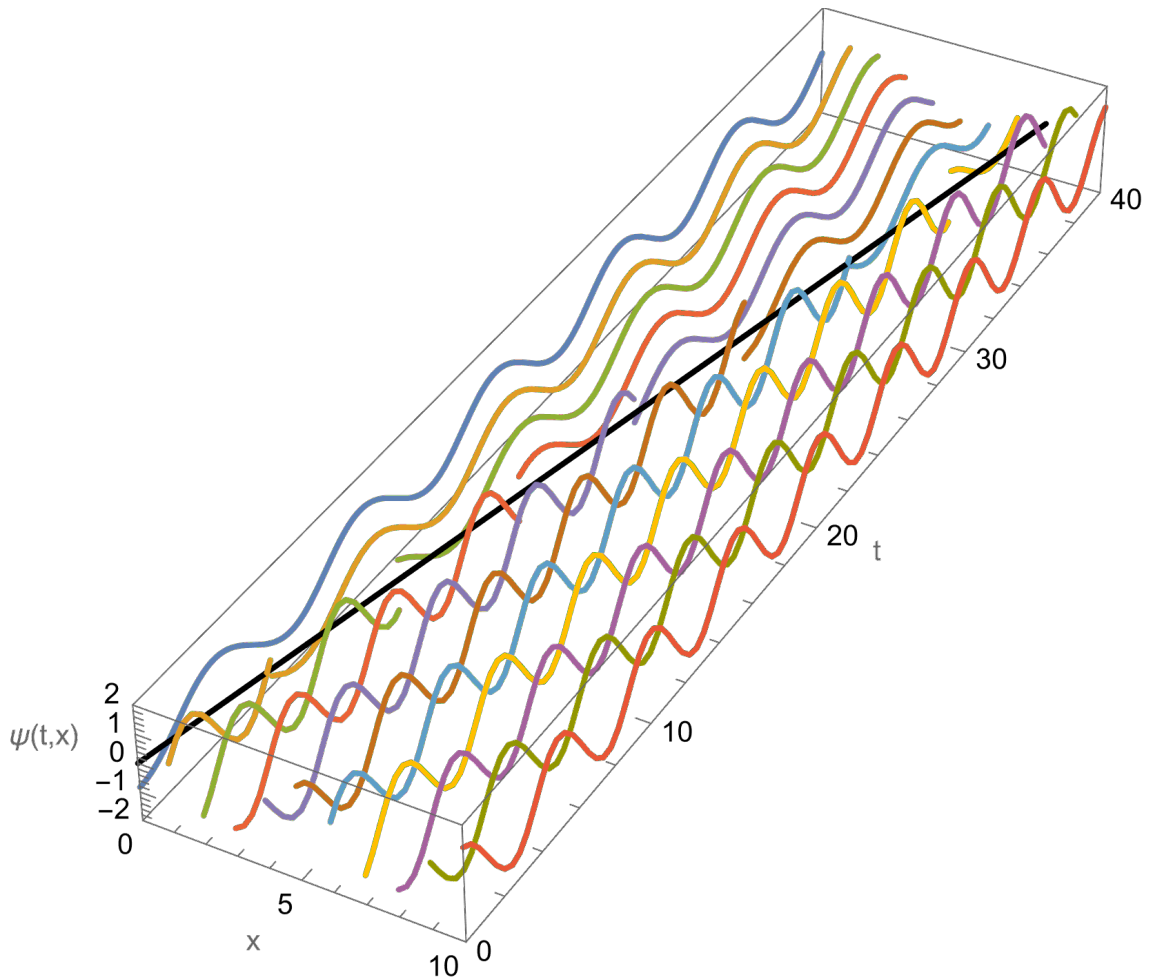


Figure 2: The solution (4.3) (or, equivalently, Eq. (4.18) in hyperboloidal coordinates), recovered with a discontinuous method of lines. The black line represents the worldline  $\zeta(t) = vt$  of the particle. Each colored line represents the solution  $\Psi(t,x)$  on the respective grid-point  $x = x_i$  as a function of time  $t$ . The solution  $\Psi(t,x)$  (and its spatial and temporal derivatives) is discontinuous across the worldline  $\zeta(t)$ , both in the space and time direction. Thus, a discontinuous collocation method is required to differentiate  $\Psi$  in the  $x$  direction, and a discontinuous time integration method is required to integrate the solution in the  $t$  direction. Specifically, every time the particle worldline crosses a grid-point, the time integrator must account for the jump in the solution and its time derivatives, as described in Sec. 3.

as the superposition  $\Psi = \Psi_H + \Psi_{NS}$ , where  $\Psi_H$  is a general solution to the homogeneous equation and  $\Psi_{NS}$  is a particular solution corresponding to the source terms. We note that, since the source terms are distributions, the part  $\Psi_{NS}$  of the target function is necessarily

non-smooth. We begin with the same decomposition of the non-smooth part of the target function,

$$\Psi_{\text{NS}}(\tau, \sigma) = \sum_{n=0}^{\infty} J_n(\tau) \Phi_n(\sigma; \zeta), \quad (4.19)$$

but now assume the more general form (4.11) for the evolution equation.

We substitute the form Eq. (4.19) into this problem and simplify the terms of the left hand side of Eq. (4.11). In evaluating the source terms on the right hand side, we now consider the possibility of  $F$  and  $G$  depending on  $\sigma$  as well as  $\tau$ , so we must invoke the  $\delta$  function *selection properties* (cf. Appendix D of [54]):

$$f(\sigma)\delta'(\sigma - \sigma_0) = f(\sigma_0)\delta'(\sigma - \sigma_0) - f'(\sigma_0)\delta(\sigma - \sigma_0) \quad (4.20)$$

$$g(\sigma)\delta(\sigma - \sigma_0) = g(\sigma_0)\delta(\sigma - \sigma_0) \quad (4.21)$$

Applied to this problem, we have

$$\begin{aligned} & F(\tau, \sigma)\delta'(\sigma - \zeta(\tau)) + G(\tau, \sigma)\delta(\sigma - \zeta(\tau)) \\ &= F(\tau, \zeta(\tau))\delta'(\sigma - \zeta(\tau)) + \left( -\partial_\sigma F(\tau, \zeta(\tau)) + G(\tau, \zeta(\tau)) \right) \delta(\sigma - \zeta(\tau)) \end{aligned} \quad (4.22)$$

The details of this calculation are presented in Appendix A. The end results are explicit expressions for the first two jumps,

$$J_0 = \gamma^2 F(\tau, \zeta) \quad (4.23)$$

$$\begin{aligned} J_1 = \gamma^2 \left( -\partial_\sigma F(\tau, \zeta) + G(\tau, \zeta) + \dot{J}_0 \left( 2Z(\zeta)\dot{\zeta} - A(\zeta) \right) \right. \\ \left. + J_0 \left( Z'(\zeta)\dot{\zeta}^2 - A'(\zeta)\dot{\zeta} + C'(\zeta) + Z(\zeta)\ddot{\zeta} + B(\zeta)\dot{\zeta} - E(\zeta) \right) \right) \end{aligned} \quad (4.24)$$

where  $\gamma$  is the Lorentz factor given by

$$\gamma^{-2} = Z(\zeta)\dot{\zeta}^2 - A(\zeta)\dot{\zeta} + C(\zeta). \quad (4.25)$$

A recursion relation specifies all higher order jumps:

$$\begin{aligned} J_{n+2} = -\gamma^2 \left( \sum_{k=0}^n \binom{n}{k} \left( A^{(k)}(\zeta) \dot{J}_{n+1-k} + B^{(k)}(\zeta) (\dot{J}_{n-k} - \dot{\zeta} J_{n+1-k}) - E^{(k)}(\zeta) J_{n+1-k} \right. \right. \\ \left. \left. + Z^{(k)}(\zeta) (\ddot{J}_{n-k} - 2\dot{J}_{n+1-k}\dot{\zeta} + J_{n+1-k}\ddot{\zeta}) \right) + \sum_{k=1}^n \binom{n}{k} J_{n+2-k} \left( A^{(k)}(\zeta)\dot{\zeta} + C^{(k)}(\zeta) \right) \right) \end{aligned} \quad (4.26)$$

The coefficients  $J_n(\tau)$  give the discontinuities in the  $n^{\text{th}}$  derivative of  $\Psi_{\text{NS}}$ . In fact, noting that  $\Phi_0(\tau, \sigma) = \frac{1}{2} \text{sgn}(\sigma - \zeta(\tau))$ ,

$$\llbracket \Psi_{\text{NS}} \rrbracket = \lim_{\sigma \rightarrow \zeta^+} \Psi_{\text{NS}}(\tau, \sigma) - \lim_{\sigma \rightarrow \zeta^-} \Psi_{\text{NS}}(\tau, \sigma) = J_0(\tau) \quad (4.27)$$

If instead we take the limits in the  $\tau$ -direction to obtain the first jump  $K_0$ , we have

$$K_0 = \lim_{\tau \rightarrow T^+} \Psi_{\text{NS}}(\tau, \sigma) - \lim_{\tau \rightarrow T^-} \Psi_{\text{NS}}(\tau, \sigma) = -J_0(T) = -\llbracket \Psi_{\text{NS}} \rrbracket, \quad (4.28)$$

where we have defined  $T = \zeta^{-1}(\sigma)$ . Thus, a jump along the  $\tau$ -direction is numerically the negative of a jump along the  $\sigma$ -direction. This observation is crucial to the application of discontinuous Hermite integrators to time evolution: once the jumps are calculated in the spatial direction, they are easily adapted to the time direction for use in Eqs. (3.6) and (3.9).

#### 4.4 Distributionally-sourced wave equation in hyperboloidal coordinates

We wish to solve Eq. (4.1) by employing hyperboloidal compactification; that is, in a coordinate system where  $\mathcal{I}^+$ , the only null boundary surface in Minkowski space, is brought to finite coordinate values. Our studies of effective action in the previous section has yielded such a coordinate transformation on Minkowski space, Eq. (4.12).

The only remaining question is how to handle the source terms in these coordinates. We wish to study Solutions I and II in [25], so we consider the particle worldline  $\zeta(t) = vt$  giving rise to the source terms  $F(t)\delta'(x - vt)$  and  $G(t)\delta(x - vt)$  in a standard Minkowski coordinate chart  $\{t, x\}$ . Since the  $\delta$ -functions are given in another chart, we bring them to the new  $\{\tau, \sigma\}$  chart by invoking the  $\delta$ -function *composition rules* (cf. Appendix D of [54]):

$$\delta(f(\sigma)) = \frac{1}{|f'(\sigma_0)|} \delta(\sigma - \sigma_0) \quad (4.29)$$

$$\delta'(f(\sigma)) = \frac{f'(\sigma_0)}{|f'(\sigma_0)|^3} \delta'(\sigma - \sigma_0) + \frac{f''(\sigma_0)}{|f'(\sigma_0)|^3} \delta(\sigma - \sigma_0) \quad (4.30)$$

where  $f(\sigma_0) = 0$ . Noting that  $x = x(\sigma)$  and  $t = t(\tau, \sigma)$ , we note that the  $\delta$ -function source terms for this problem transform as

$$G(t)\delta(x - vt) = \frac{G(t_\zeta)}{|\Delta(\zeta)|} \delta(\sigma - \zeta) \quad (4.31)$$

$$F(t)\delta'(x - vt) = \frac{\Delta(\zeta)}{|\Delta(\zeta)|^3} F(t_\zeta) \delta'(\sigma - \zeta) + \left( \frac{\Delta'(\zeta)}{|\Delta(\zeta)|^3} F(t_\zeta) - \frac{\Delta(\zeta)}{|\Delta(\zeta)|^3} F'(t_\zeta) \frac{\partial t}{\partial \sigma} \Big|_{\zeta} \right) \delta(\sigma - \zeta) \quad (4.32)$$

where we have invoked both the selection and composition properties of the  $\delta$ -function and we have let  $\sigma = \zeta(\tau)$  be the worldline of the particle ( $x = vt = \zeta(t)$ ) transformed to the new coordinate chart  $\{\tau, \sigma\}$ . For convenience we have also defined

$$\Delta(\zeta) = \frac{\partial}{\partial \sigma}(x - vt) \Big|_{\sigma=\zeta} \quad (4.33)$$

and

$$t_\zeta = t(\tau, \zeta(\tau)). \quad (4.34)$$

The particle position in the chart (4.13) is governed by the equation of motion

$$\frac{d\zeta}{d\tau} = \frac{2v(1-\zeta)\zeta^2}{1+v(1-2\zeta^2)}. \quad (4.35)$$

which may be solved to give  $\zeta(\tau)$  either implicitly or numerically. We further note that, in this chart,

$$\Delta(\zeta) = \frac{1+v(1-2\zeta^2)}{2\zeta^2(1-\zeta)}. \quad (4.36)$$

and

$$t_\zeta = \frac{1+2\zeta \tanh^{-1}(1-2\zeta)}{2v\zeta} \quad (4.37)$$

This information now allows us to completely determine the jumps in both Solutions I (Eq. (4.2) and II (Eq. (4.3)) using the generalized recursion relation. The first few are tabulated in Appendix B.

Next, we incorporate the transformed  $\delta$ -function source terms in the same manner as in Ref. [50]. For generality, we suppose that the wave equation is written in the form of Eq. (4.11) which, upon first order in time reduction, takes the form:

$$\begin{cases} \partial_\tau \Psi - \Pi = \tilde{F}(\tau) \delta(\sigma - \zeta) \\ Z(\sigma) \partial_\tau \Pi + A(\sigma) \partial_\sigma \Pi + B(\sigma) \Pi + C(\sigma) \partial_\sigma^2 \Psi + E(\sigma) \partial_\sigma \Psi = \tilde{G}(\tau) \delta(\sigma - \zeta) \end{cases} \quad (4.38)$$

Here, to avoid the difficulty of a  $\delta'$  function in a first-order equation, we have defined the variable  $\Pi$  by

$$\partial_\tau \Psi - \Pi = \frac{\Delta(\zeta)}{|\Delta(\zeta)|^3} \frac{F(t_\zeta)}{A(\zeta) - \zeta Z(\zeta)} \delta(\sigma - \zeta) := \tilde{F}(\tau) \delta(\sigma - \zeta). \quad (4.39)$$

Substitution of  $\Pi$  into the field equation (4.11) yields an equation that is first-order in  $\Psi, \Pi$  given by

$$\begin{aligned} & Z(\sigma) \partial_\tau \Pi + A(\sigma) \partial_\sigma \Pi + B(\sigma) \Pi + C(\sigma) \partial_\sigma^2 \Psi + E(\sigma) \partial_\sigma \Psi \\ &= \left( \frac{\Delta'(\zeta)}{|\Delta(\zeta)|^3} F(t_\zeta) - \frac{\Delta(\zeta)}{|\Delta(\zeta)|^3} F'(t_\zeta) \frac{\partial t}{\partial \sigma} \Big|_\zeta + \frac{G(t_\zeta)}{|\Delta(\zeta)|} - Z(\zeta) \tilde{F}'(\tau) \right. \\ & \quad \left. - (A'(\zeta) - \zeta Z'(\zeta)) \tilde{F}(\tau) \right) \delta(\sigma - \zeta) := \tilde{G}(\tau) \delta(\sigma - \zeta) \quad (4.40) \end{aligned}$$



We proceed to demonstrate that the discontinuous collocation methods of Section 2 with the discontinuous time integration methods of Section 3 may be used in concert to solve Eq. (4.14) with distributional source terms Eqs. (4.31) and (4.32). Before doing so, we first take the time integration method used in Section 4 and reformulate it using a first-order in time “state vector” approach so as to simplify the matrix equations used in evolution. Since the target function is now discontinuous, there is the added complication of correcting the spatial derivative operators in Eq. (4.38).

We observe that discontinuous corrections only enter as a consequence of the  $A, C$ , and  $E$  coefficients. Using Eq. (2.13), we note that the above-mentioned terms discretize to

$$E(\sigma)\partial_\sigma\Psi|_{\sigma=\sigma_i} \simeq \sum_{j=0}^N \left( \mathbf{E}\mathbf{D}^{(1)} \right)_{ij} [\Psi_j + \Delta(\sigma_j - \zeta; \sigma_i - \zeta)], \quad \mathbf{E} = \text{diag}(E(\sigma_i)) \quad (4.41)$$

$$C(\sigma)\partial_\sigma^2\Psi|_{\sigma=\sigma_i} \simeq \sum_{j=0}^N \left( \mathbf{C}\mathbf{D}^{(2)} \right)_{ij} [\Psi_j + \Delta(\sigma_j - \zeta; \sigma_i - \zeta)], \quad \mathbf{C} = \text{diag}(C(\sigma_i)) \quad (4.42)$$

$$A(\sigma)\partial_\sigma\Pi|_{\sigma=\sigma_i} \simeq \sum_{j=0}^N \left( \mathbf{A}\mathbf{D}^{(1)} \right)_{ij} [\Pi_j + \Delta_\Pi(\sigma_j - \zeta; \sigma_i - \zeta)], \quad \mathbf{A} = \text{diag}(A(\sigma_i)) \quad (4.43)$$

where an inner (or dot) product between  $\mathbf{E}, \mathbf{C}, \mathbf{A}$  and the differentiation matrices  $\mathbf{D}^{(n)}$  is implied.

This indicates that the discretized Eq. (4.38) should now include an effective source term of the form

$$\mathbf{s}(\tau) = \left( \mathbf{r}^A(\tau) + \mathbf{s}^C(\tau) + \mathbf{s}^E(\tau) \right) \quad (4.44)$$

where

$$s_i^E(\tau) = \sum_{j=0}^N \left( \mathbf{E}\mathbf{D}^{(1)} \right)_{ij} \Delta(\sigma_j - \zeta; \sigma_i - \zeta) \quad (4.45)$$

$$s_i^C(\tau) = \sum_{j=0}^N \left( \mathbf{C}\mathbf{D}^{(2)} \right)_{ij} \Delta(\sigma_j - \zeta; \sigma_i - \zeta) \quad (4.46)$$

$$r_i^A(\tau) = \sum_{j=0}^N \left( \mathbf{A}\mathbf{D}^{(1)} \right)_{ij} \Delta_\Pi(\sigma_j - \zeta; \sigma_i - \zeta) \quad (4.47)$$

Note that  $\Delta_\Pi$  is defined in the same manner as Eq. (2.9), but now the  $\kappa$  function is calculated using the jumps in  $\Pi$  instead of  $\Psi$ .

Putting everything together, the evolution equation (4.38) for the discretized state vector becomes

$$\frac{d\mathbf{u}}{d\tau} = \mathbf{L}\mathbf{u} + \mathbf{s}(\tau) + \tilde{\mathbf{F}}(\tau)\delta(\sigma - \zeta) \quad (4.48)$$

where

$$\mathbf{u}(\tau) = \begin{pmatrix} \Psi(\tau) \\ \Pi(\tau) \end{pmatrix}, \quad \tilde{\mathbf{F}}(\tau) = \begin{pmatrix} \tilde{F}(\tau) \\ \tilde{G}(\tau) \end{pmatrix} \quad (4.49)$$

and  $\delta(\sigma - \zeta)$  is a shorthand for a vector whose elements are  $\delta(\sigma_i - \zeta)$  (*i.e.* a list of  $\delta$  functions that “turn on” the coefficients whenever the particle worldline  $\zeta(\tau)$  crosses a grid point  $\sigma_i$ ). Here, the product  $\tilde{\mathbf{F}}(\tau)\delta(\sigma - \zeta) = \tilde{\mathbf{F}}(\tau) \circ \delta(\sigma - \zeta)$  is the Hadamard (or element-wise) product of two vectors, while  $\mathbf{L}\mathbf{u}$  is the inner (or dot) product of a matrix and a vector.

We now pose Eq. (4.48) as an integral equation over an interval  $[\tau_\nu, \tau_{\nu+1}]$ :

$$\mathbf{u}^{\nu+1} = \mathbf{u}^\nu + \mathbf{L} \int_{\tau_\nu}^{\tau_{\nu+1}} \mathbf{u}(\tau) d\tau + \int_{\tau_\nu}^{\tau_{\nu+1}} \mathbf{s}(\tau) d\tau + \int_{\tau_\nu}^{\tau_{\nu+1}} \tilde{\mathbf{F}}(\tau) \delta(\sigma - \zeta) d\tau \quad (4.50)$$

and demonstrate that discontinuous Hermite integration may be applied to numerically solve this equation for both Solutions I and II.

#### 4.4.1 Discontinuous trapezium rule

We first apply the discontinuous trapezium rule DH2 (Eq. (3.6)) to approximate the above integrals, so

$$\mathbf{u}^{\nu+1} = \mathbf{u}^\nu + \frac{\Delta\tau}{2} \mathbf{L}(\mathbf{u}^\nu + \mathbf{u}^{\nu+1}) + \mathbf{K}_{\text{H2}}(\Delta\tau, \Delta\tau_i) + \frac{\Delta\tau}{2} (\mathbf{s}^\nu + \mathbf{s}^{\nu+1}) + \llbracket \mathbf{u} \rrbracket \quad (4.51)$$

where

$$\llbracket \mathbf{u} \rrbracket = \int_{\tau_\nu}^{\tau_{\nu+1}} \tilde{\mathbf{F}}(\tau) \delta(\sigma - \zeta) d\tau = \frac{1}{|d\zeta/d\tau|_{\tau_i}} \tilde{\mathbf{F}}(\tau_i) \theta(\tau_{\nu+1} - \tau_i) \theta(\tau_i - \tau_\nu) \quad (4.52)$$

is a function that turns on when the worldline  $\zeta(\tau)$  crosses the gridpoint  $\sigma_i$  to alter the value of  $u_i$  and  $\mathbf{K}_{\text{H2}}(\Delta\tau, \Delta\tau_i)$  is a vector including the jumps in  $\mathbf{u}$  which appear in Eq. (3.6);  $\Delta\tau_i = \tau_i - \tau_\nu$  represents the interval from  $\tau_\nu$  to the crossing time  $\tau_i$  satisfying  $\zeta(\tau_i) = \sigma_i$  for some  $i$ , if such a time exists in the interval  $[\tau_\nu, \tau_{\nu+1}]$ . This algebraic equation may be solved for  $\mathbf{u}^{\nu+1} = \mathbf{u}(\tau_{\nu+1})$  using the methods of [50] to arrive at a form which mitigates round-off error:

$$\mathbf{u}^{\nu+1} = \mathbf{u}^\nu + \left( \mathbf{I} - \frac{\Delta\tau}{2} \mathbf{L} \right)^{-1} \left( \Delta\tau \mathbf{L} \mathbf{u}^\nu + \mathbf{K}_{\text{H2}}(\Delta\tau, \Delta\tau_i) + \frac{\Delta\tau}{2} (\mathbf{s}^\nu + \mathbf{s}^{\nu+1}) + \llbracket \mathbf{u} \rrbracket \right) \quad (4.53)$$

As discussed in Section 3, such a scheme should exhibit second order convergence in  $\Delta\tau$ .

#### 4.4.2 Discontinuous Hermite rule

We next apply the discontinuous Hermite rule DH4 (Eq. (3.9)) to the above integrals and find that

$$\begin{aligned} \mathbf{u}^{\nu+1} = \mathbf{u}^\nu + \frac{\Delta\tau}{2} \mathbf{L}(\mathbf{u}^\nu + \mathbf{u}^{\nu+1}) + \frac{\Delta\tau^2}{12} \mathbf{L}(\dot{\mathbf{u}}^\nu - \dot{\mathbf{u}}^{\nu+1}) + \mathbf{K}_{\text{H4}}(\Delta\tau, \Delta\tau_i) \\ + \frac{\Delta\tau}{2} (\mathbf{s}^\nu + \mathbf{s}^{\nu+1}) + \frac{\Delta\tau^2}{12} (\dot{\mathbf{s}}^\nu - \dot{\mathbf{s}}^{\nu+1}) + \llbracket \mathbf{u} \rrbracket \end{aligned} \quad (4.54)$$

where now  $\mathbf{K}_{\text{H4}}(\Delta\tau, \Delta\tau_i)$  is a vector including the jumps in  $\mathbf{u}$  which appear in Eq. (3.9). The  $\tau$ -derivatives of  $\mathbf{u}$  represented by the overdot may be removed by using the original

evolution equation Eq. (4.48). The resulting algebraic equation may be solved for  $\mathbf{u}^{\nu+1}$  using the same method as [50]:

$$\begin{aligned} \mathbf{u}^{\nu+1} = \mathbf{u}^{\nu} + & \left( \mathbf{I} - \frac{\Delta\tau}{2} \mathbf{L} \left( \mathbf{I} - \frac{\Delta\tau}{6} \mathbf{L} \right) \right)^{-1} \left( \Delta\tau \mathbf{L} \left( \mathbf{u}^{\nu} + \frac{\Delta\tau}{12} (\mathbf{s}^{\nu} - \mathbf{s}^{\nu+1}) \right) \right. \\ & \left. + \mathbf{K}_{\text{H4}}(\Delta\tau, \Delta\tau_i) + \frac{\Delta\tau}{2} (\mathbf{s}^{\nu} + \mathbf{s}^{\nu+1}) + \frac{\Delta\tau^2}{12} (\dot{\mathbf{s}}^{\nu} - \dot{\mathbf{s}}^{\nu+1}) + \llbracket \mathbf{u} \rrbracket \right) \end{aligned} \quad (4.55)$$

In the above formula, terms polynomial in  $\Delta\tau$  have been factored in Horner form to improve arithmetic precision.

We've replaced matrix multiplications with separate matrix multiplication and addition steps to reduce round-off error accumulation, as shown by prior work [51, 54]. This enhances numerical energy and phase-space volume conservation. Modern CPU and GPU libraries accelerate these operations, allowing efficient implementation without intensive programming. Given their conservation qualities, reduced errors, and library support, these time-symmetric schemes excel in long-term evolution of distributionally sourced PDEs, like those in black hole perturbation theory and Extreme Mass Ratio Inspirational simulations. We now present numerical results.

#### 4.4.3 Numerical results

With these two integration rules, we may now numerically integrate Eq. (4.38) in a hyperboloidal coordinate chart and compare to Solutions I and II given by Eqs. (4.17) and (4.18) respectively. We take as initial data each solution evaluated at  $\tau_0$  satisfying  $t(\tau_0, \zeta(\tau_0)) = 0$ .

Our schemes work for both finite-difference and pseudo-spectral methods. For instance, interpolation on Chebyshev-Gauss-Lobatto nodes

$$\sigma_i = \frac{a+b}{2} + \frac{b-a}{2} z_i, \quad z_i = -\cos\theta_i, \quad \theta_i = \frac{i\pi}{N}, \quad i = 0, 1, \dots, N \quad (4.56)$$

converges uniformly for every absolutely continuous function [9]. If all the function derivatives are bounded on the interval  $x \in [a, b]$ , Chebyshev interpolation has the property of exponential convergence on the interval  $x \in [a, b]$ . In Section (2), we generalized this concept to piecewise smooth functions. The elements  $D_{ij}$  of the  $(N+1) \times (N+1)$  Chebyshev first derivative matrix  $D$  are given by

$$D_{ij}^{(1)} = \frac{2}{b-a} \begin{cases} \frac{c_i(-1)^{i+j}}{c_j(z_i - z_j)} & i \neq j \\ \frac{z_i}{2(1-z_i^2)} & i = j \neq 0, N \\ -\frac{2N^2+1}{6} & i = j = 0 \\ \frac{2N^2+1}{6} & i = j = N \end{cases} \quad (4.57)$$

where  $c_0 = c_N = 2$  and  $c_1, \dots, c_{N-1} = 1$ . The second derivative operator can be evaluated by

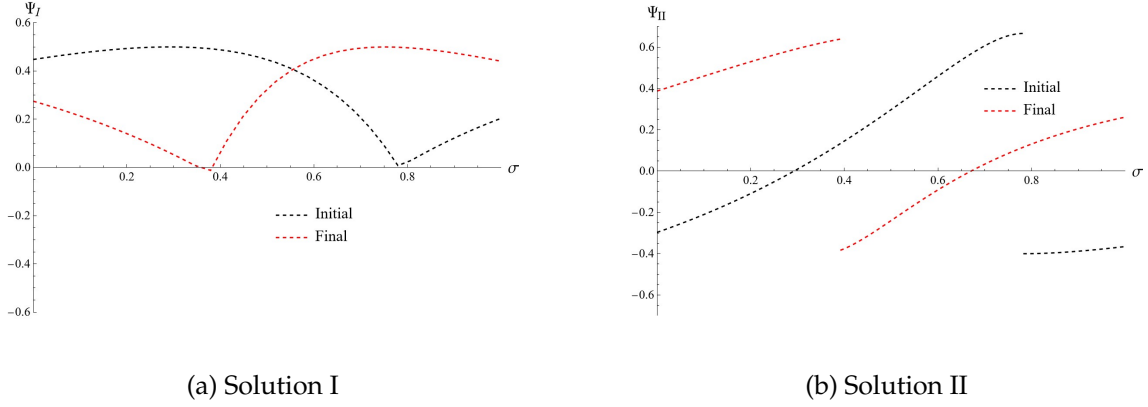
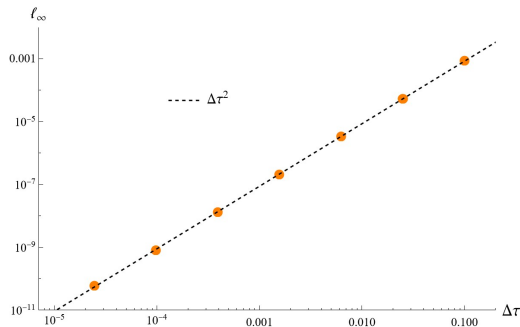


Figure 3: Numerical solutions to Eq. (4.40) using discontinuous collocation methods for spatial discretization and the discontinuous trapezoidal rule in Eq. (3.6) for time integration. The Initial function was selected to be the exact solutions provided in [25] at  $\tau = \tau_0$ ; this ensures the numerical solution can be directly compared to an exact solution when studying convergence. We evolved the reduced system from  $\tau = \tau_0$  to  $\tau = 4.3$  taking  $\Delta\tau = 0.05$ .

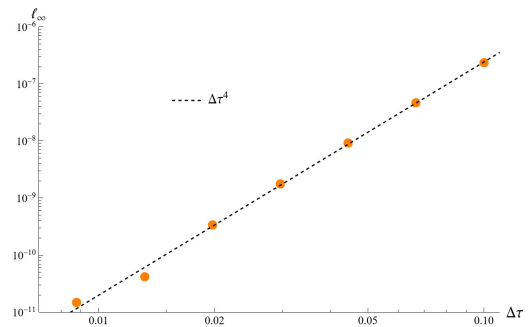
$\mathbf{D}^{(2)} = (\mathbf{D}^{(1)})^2$  or, equivalently [18],

$$D_{ij}^{(2)} = \left( \frac{2}{b-a} \right)^2 \begin{cases} \frac{(-1)^{i+j}}{c_j} \frac{z_i^2 + z_i z_j - 2}{(1-z_i^2)(z_i - z_j)^2} & i \neq 0, i \neq N, i \neq j \\ -\frac{(N^2-1)(1-z_i^2)+3}{3(1-z_i^2)^2} & i \neq 0, i \neq N, i = j \\ \frac{2}{3} \frac{(-1)^i (2N^2+1)(1-z_i)-6}{c_i (1-z_i)^2} & i = 0, j \neq 0 \\ \frac{2}{3} \frac{(-1)^{i+N} (2N^2+1)(1+z_i)-6}{c_i (1+z_i)^2} & i = N, j \neq N \\ -\frac{N^4-1}{15} & i = j = 0, i = j = N \end{cases} . \quad (4.58)$$

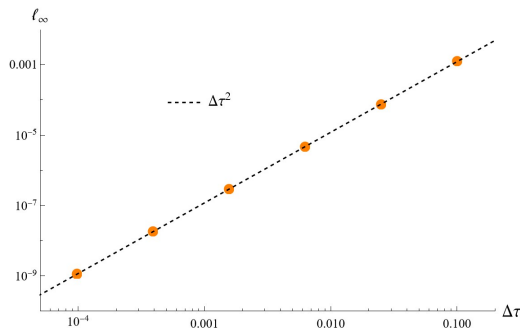
Here, we use a Chebyshev pseudo-spectral method (Eqs. (4.56) - (4.58)) to discretize the spatial interval  $\sigma \in [0, 1]$  with  $N = 45$  nodes and use  $\simeq 10-12$  jumps for each solution. The results for the discontinuous trapezium rule when  $\Delta\tau = 0.05$  are plotted in Figure 3. Moreover, we observe the expected convergence for each discontinuous method as illustrated in Figure 4.



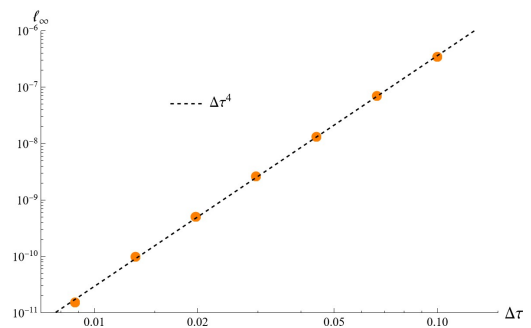
(a) DH2 Temporal Convergence, Solution I



(b) DH4 Temporal Convergence, Solution I



(c) DH2 Temporal Convergence, Solution II



(d) DH4 Temporal Convergence, Solution II

Figure 4: The  $l_\infty$  error norm of the numerical approximation to Solutions I (Eq. (4.17)) and II (Eq. (4.18)) using discontinuous collocation and numerical integration. In both cases, the discontinuous DH2 method error scales as  $\Delta\tau^2$  and the discontinuous DH4 method error scales as  $\Delta\tau^4$ , as expected.

## Acknowledgments

We thank Charles F. Gammie for co-supervising the first author's PhD dissertation [54], where the present work originally appeared. We thank Leor Barack for discontinuous second-order finite-differencing schemes and systematized spatial derivative jump calculations that inspired this work. We thank Pablo Brubeck for notes on using the Frobenius method to compute recursion relations between spatial derivative jumps, and for noticing that the original discontinuous collocation method converged for stationary but not for moving distributional sources; this observation motivated the creation of discontinuous time integration methods. We thank Garbielle Allen and Ed Seidel for support at NCSA. We thank John L. Friedman for valuable discussions on symplecticity and volume preserv-

ing and for suggesting a discontinuous method-of-lines graph. We thank Anil Zenginoğlu and Juan A. Valiente-Kroon for insights into hyperboloidal slicing and Rodrigo Panoso Macedo for suggestions and discussions on the minimal gauge. We thank Lidia Gomes Da Silva for discussions and efforts to verify our results.

## Appendix

### A Derivation of the recursion relation

We proceed by a method of undetermined coefficients assuming the form of Eq. (4.19) with the goal of determining the  $J_n(\tau)$ . We first note that the properties of the unit jump functions (*cf.* [50]) give rise to the following identities:

$$\partial_\sigma \Psi_{\text{NS}} = \sum_{n=0}^{\infty} J_{n+1}(\tau) \Phi_n(\sigma; \zeta) + J_0(\tau) \delta(\sigma - \zeta) \quad (\text{A.1})$$

$$\partial_\sigma^2 \Psi_{\text{NS}} = \sum_{n=0}^{\infty} J_{n+2}(\tau) \Phi_n(\sigma; \zeta) + J_1(\tau) \delta(\sigma - \zeta) + J_0(\tau) \delta'(\sigma - \zeta) \quad (\text{A.2})$$

$$\partial_\tau \Psi_{\text{NS}} = \sum_{n=0}^{\infty} \left( \dot{J}_n(\tau) - J_{n+1}(\tau) \dot{\zeta} \right) \Phi_n(\sigma; \zeta) - J_0(\tau) \dot{\zeta} \delta(\sigma - \zeta) \quad (\text{A.3})$$

$$\begin{aligned} \partial_\tau^2 \Psi_{\text{NS}} = \sum_{n=0}^{\infty} \left( \ddot{J}_n(\tau) - 2\dot{J}_{n+1}(\tau) \dot{\zeta} - J_{n+1}(\tau) \ddot{\zeta} + J_{n+2}(\tau) \dot{\zeta}^2 \right) \Phi_n(\sigma; \zeta) + J_0(\tau) \dot{\zeta}^2 \delta'(\sigma - \zeta) \\ + \left( J_1(\tau) \dot{\zeta}^2 - J_0(\tau) \ddot{\zeta} - 2\dot{J}_0(\tau) \dot{\zeta} \right) \delta(\sigma - \zeta) \end{aligned} \quad (\text{A.4})$$

$$\begin{aligned} \partial_\sigma \partial_\tau \Psi_{\text{NS}} = \sum_{n=0}^{\infty} \left( \dot{J}_{n+1}(\tau) - J_{n+2}(\tau) \dot{\zeta} \right) \Phi_n(\sigma; \zeta) + \left( \dot{J}_0(\tau) - J_1(\tau) \dot{\zeta} \right) \delta(\sigma - \zeta) \\ - J_0(\tau) \dot{\zeta} \delta'(\sigma - \zeta) \end{aligned} \quad (\text{A.5})$$

Upon substitution into the left hand side of Eq. (4.11), the “product rule” of [54] allows each term to be transformed into a pure expansion in jump functions.

$$E(\sigma) \partial_\sigma \Psi_{\text{NS}} = \sum_{n=0}^{\infty} \left( \sum_{l=0}^n \binom{n}{l} E^{(l)}(\zeta) J_{n+1-l}(\tau) \right) \Phi_n(\sigma; \zeta) + E(\zeta) J_0(\tau) \delta(\sigma - \zeta) \quad (\text{A.6})$$

$$\begin{aligned} C(\sigma) \partial_\sigma^2 \Psi_{\text{NS}} = \sum_{n=0}^{\infty} \left( \sum_{l=0}^n \binom{n}{l} C^{(l)}(\zeta) J_{n+2-l}(\tau) \right) \Phi_n(\tau, \sigma) \\ + \left( C(\zeta) J_1(\tau) - C'(\zeta) J_0(\tau) \right) \delta(\sigma - \zeta) + C(\zeta) J_0(\tau) \delta'(\sigma - \zeta) \end{aligned} \quad (\text{A.7})$$

$$B(\sigma)\partial_\tau\Psi_{\text{NS}} = \sum_{n=0}^{\infty} \left( \sum_{l=0}^n \binom{n}{l} B^{(l)}(\zeta) \left( \dot{J}_{n-l}(\tau) - \dot{\zeta} J_{n+1-l}(\tau) \right) \right) \Phi_n(\sigma, \zeta) - B(\zeta) J_0(\tau) \dot{\zeta} \delta(\sigma - \zeta) \quad (\text{A.8})$$

$$\begin{aligned} Z(\sigma)\partial_\tau^2\Psi_{\text{NS}} &= \sum_{n=0}^{\infty} \left( \sum_{l=0}^n \binom{n}{l} Z^{(l)}(\zeta) \left( \ddot{J}_{n-l}(\tau) - 2\dot{J}_{n+1-l}(\tau)\dot{\zeta} - J_{n+1-l}(\tau)\ddot{\zeta} + J_{n+2-l}(\tau)\dot{\zeta}^2 \right) \right) \Phi_n(\sigma; \zeta) \\ &\quad + Z(\zeta) J_0(\tau) \dot{\zeta}^2 \delta'(x - \zeta) + \left( Z(\zeta) (J_1(\tau) \dot{\zeta}^2 - J_0(\tau) \ddot{\zeta} - 2\dot{J}_0(\tau) \dot{\zeta}) \right. \\ &\quad \left. - Z'(\zeta) J_0(\tau) \dot{\zeta}^2 \right) \delta(\sigma - \zeta) \quad (\text{A.9}) \end{aligned}$$

$$\begin{aligned} A(\sigma)\partial_\tau\partial_\sigma\Psi_{\text{NS}} &= \sum_{n=0}^{\infty} \left( \sum_{l=0}^n \binom{n}{l} A^{(l)}(\zeta) \left( \dot{J}_{n+1-l}(\tau) - J_{n+2-l}(\tau)\dot{\zeta} \right) \right) \Phi_n(\sigma; \zeta) \\ &\quad + \left( A(\zeta) (\dot{J}_0(\tau) - J_1(\tau)\dot{\zeta}) - A'(\zeta) J_0(\tau) \right) \delta(x - \zeta) - J_0(\tau) A(\zeta) \dot{\zeta} \delta'(\sigma - \zeta) \quad (\text{A.10}) \end{aligned}$$

These expressions are then substituted into the left hand side of Eq. (4.11). Equating the coefficients of  $\delta'(\sigma - \zeta)$  and  $\delta(\sigma - \zeta)$  results in Eqs. (4.23) and (4.24), respectively. To obtain the recursion relation of Eq. (4.26), observe that the coefficients of each remaining  $\Phi_n$  must vanish and identify the terms proportional to  $J_{n+2}(\tau)$  in each sum over  $l$ .

## B Jump expressions

We present the first few jumps of Solutions I and II when transformed to the hyperboloidal coordinate chart of Eqs. (4.9) and (4.10). These expressions follow from generalized jump conditions of Eqs. (4.23), (4.24), and (4.26) along with the transformed source terms of Eqs. (4.31) and (4.32). The first few jumps of Solution I are

$$J_0 = 0 \quad (\text{B.1a})$$

$$J_1 = -\frac{1-v(1-2\zeta^2)}{2(1-v^2)(1-\zeta)\zeta^2} \text{cost}_\zeta \quad (\text{B.1b})$$

$$J_2 = \frac{1}{2} \left( \frac{2+\zeta}{(1+v)\zeta^3} - \frac{1}{(1-v)(1-\zeta)^2} \right) \text{cost}_\zeta - \frac{(1-v-2\zeta^2)(1-v+2\zeta^2)}{2(1-v^2)^2(1-\zeta)^2\zeta^4} \text{sint}_\zeta \quad (\text{B.1c})$$

$$\begin{aligned} J_3 &= \frac{-3(1-v)^3(4v^2+8v+3)\zeta^4 - 3(1-v)^3(2v^2+4v+3)\zeta^2 + (-4v^5+10v^3+2v)\zeta^6}{2(1-v)^3(1+v)^3(1-\zeta)^3\zeta^6} \\ &\quad + \frac{16(1-v)^3(1+v)^2\zeta^3 + (1-v)^3}{2} \text{cost}_\zeta + \frac{3}{2} \left( \frac{(1+\zeta)(2+\zeta)}{(1+v)^2\zeta^5} + \frac{1}{(1-v)^2(1-\zeta)^3} \right) \text{sint}_\zeta \quad (\text{B.1d}) \end{aligned}$$

$$J_4 = 3 \left( -\frac{2+\zeta(5-v(v+2)\zeta(4+\zeta))}{(1+v)^2\zeta^5} + \frac{v(2-v)}{(1-v)^3(1-\zeta)^4} \right) \text{cost}_\zeta \\ + \frac{1}{2} \left( \frac{-11(2-v)v+10}{(1-v)^4(1-\zeta)^4} + \frac{\zeta(\zeta(-11v(v+2)+10)\zeta(\zeta+4)-6(6v(v+2)+5))+4+1}{(1+v)^4\zeta^8} \right) \text{sint}_\zeta \quad (\text{B.1e})$$

$$J_5 = \frac{1}{2} \left( \frac{-10(2-v)v(24(2-v)v+13)}{(1-v)^5(1-\zeta)^5} + \frac{\zeta(\zeta(\zeta(-(v(2+v)(24v(v+2)+13)-10)\zeta(\zeta+5) \right. \\ \left. +260v(2+v)+250)+120v(2+v)+110)-5)-1}{(1+v)^5\zeta^{10}} \right) \text{cost}_\zeta \\ + 5 \left( \frac{5(2-v)v-4}{(1-v)^4(\zeta-1)^5} + \frac{\zeta(\zeta((5v(v+2)+4)\zeta(\zeta+5)+3(8v(v+2)+5))-7)-2}{(v+1)^4\zeta^9} \right) \text{sint}_\zeta \quad (\text{B.1f})$$

$$J_6 = \frac{15}{2} \left( \frac{(2-v)v(1-8(2-v)v)-6}{(1-v)^5(1-\zeta)^6} + \frac{\zeta(\zeta((v(v+2)(8v(v+2)+1)-6)(\zeta+6)\zeta^2 \right. \\ \left. -14(11v(v+2)+10)\zeta-80v(v+2)-64)+9)+2}{(v+1)^5\zeta^{11}} \right) \text{cost}_\zeta \\ + \frac{1}{2} \left( \frac{190-(2-v)v(463-274v(2-v))}{(1-v)^6(1-\zeta)^6} + \frac{\zeta(\zeta(\zeta(\zeta(-(v(v+2)(274v(v+2)+463) \right. \\ \left. +190)\zeta(\zeta+6)-15(v(v+2)(120v(v+2)+169)+50))+940v(v+2)+920) \right. \\ \left. +300v(v+2)+285)-6)-1}{(v+1)^6\zeta^{12}} \right) \text{sint}_\zeta \quad (\text{B.1g})$$

The first few jumps of Solution II are

$$J_0 = -\frac{\text{cost}_\zeta}{1-v^2} \quad (\text{B.2a})$$

$$J_1 = \frac{2(1+v^2)\zeta^2-(1-v^2)}{2(1-v^2)^2\zeta^2(1-\zeta)} \text{sint}_\zeta \quad (\text{B.2b})$$

$$J_2 = \frac{1}{2} \left( \frac{(1+\zeta)^2}{(1+v)^3\zeta^4} + \frac{1}{(1-v)^3(1-\zeta)^2} \right) \text{cost}_\zeta + \frac{1}{2} \left( \frac{2+\zeta}{(1+v)^2\zeta^3} + \frac{1}{(1-v)^2(1-\zeta)^2} \right) \text{sint}_\zeta \quad (\text{B.2c})$$

$$J_3 = \frac{3}{2} \left( -\frac{(1+\zeta)(2+\zeta)}{(1+v)^3\zeta^5} + \frac{1}{(1-v)^3(1-\zeta)^3} \right) \text{cost}_\zeta \\ + \frac{1}{2} \left( \frac{1-2v(2-v)}{(1-v)^4(1-\zeta)^3} + \frac{\zeta(3-(2v(v+2)+1)\zeta(\zeta+3))+1}{(v+1)^4\zeta^6} \right) \text{sint}_\zeta \quad (\text{B.2d})$$



$$J_4 = \frac{1}{2} \left( \frac{10 - 11v(2-v)}{(1-v)^5(1-\zeta)^4} + \frac{\zeta(\zeta((11v(v+2)+10)\zeta(\zeta+4)+6(6v(v+2)+5))-4)-1}{(v+1)^5\zeta^8} \right) \cos t_\zeta \\ + 3 \left( -\frac{v(2-v)}{(1-v)^4(1-\zeta)^4} + \frac{\zeta(v(v+2)\zeta(\zeta+4)-5)-2}{(v+1)^4\zeta^7} \right) \sin t_\zeta \quad (\text{B.2e})$$

$$J_5 = 5 \left( -\frac{5(2-v)v+4}{(1-v)^5(1-\zeta)^5} + \frac{\zeta(\zeta(-(5v(v+2)+4)\zeta(\zeta+5)-3(8v(v+2)+5))+7)+2}{(v+1)^5\zeta^9} \right) \cos t_\zeta \\ + \frac{1}{2} \left( \frac{-10+v(2-v)(24v(2-v)v-13)}{(1-v)^6(1-\zeta)^5} + \frac{\zeta(\zeta(\zeta(-(v(v+2)(24v(v+2)+13)-10)\zeta(\zeta+5) \right. \\ \left. +260v(v+2)+250)+120v(v+2)+110)-5)-1}{(v+1)^6\zeta^{10}} \right) \sin t_\zeta \quad (\text{B.2f})$$

$$J_6 = \frac{1}{2} \left( \frac{\zeta(\zeta(\zeta((v(v+2)(274v(v+2)+463)+190)(\zeta+6)\zeta^2+15(v(v+2)(120v(v+2)+169) \right. \\ \left. +50)\zeta-940v(v+2)-920)-15(20v(v+2)+19))+6)+1}{(v+1)^7\zeta^{12}} \right. \\ \left. - \frac{v(2-v)(-274v(2-v)+463)+190}{(1-v)^7(1-\zeta)^6} \right) \cos t_\zeta + \frac{15}{2} \left( \frac{(v-2)v(8(v-2)v+1)-6}{(1-v)^6(1-\zeta)^6} \right. \\ \left. + \frac{\zeta(\zeta((v(v+2)(8v(v+2)+1)-6)(\zeta+6)\zeta^2-14(11v(v+2)+10)\zeta}{(v+1)^6\zeta^{11}} \right. \\ \left. \left. - \frac{80v(v+2)-64+9)+2}{(v+1)^6\zeta^{11}} \right) \sin t_\zeta \quad (\text{B.2g})$$

## C Time Jumps

As shown in Eqs. (4.27)-(4.28), these same jumps may be used to determine the  $\tau$ -direction jumps needed for the discontinuous Hermite integration schemes up to a sign. We already showed that

$$K_0(\zeta) = -J_0(T). \quad (\text{C.1})$$

where  $T = \zeta^{-1}(\sigma)$  as before. We go further by noting that Eq. (A.3) implies

$$K_1(\zeta) = -(\dot{J}_0(T) - \dot{\zeta} J_1(T)) \quad (\text{C.2})$$

and Eq. (A.4) implies

$$K_2(\zeta) = -(\ddot{J}_0(T) - 2\dot{J}_1(T)\dot{\zeta} - J_1(T)\ddot{\zeta} + J_2(T)\dot{\zeta}^2) \quad (\text{C.3})$$

To determine  $K_3$ , differentiate Eq. (A.4) and negate the coefficient of  $\Phi_0$  to find

$$K_3(\zeta) = -(\ddot{\ddot{J}}_0(T) - 3\ddot{J}_1(T)\dot{\zeta} - 3\dot{J}_1(T)\ddot{\zeta} - J_1(T)\ddot{\ddot{\zeta}} + 3\dot{J}_2(T)\dot{\zeta}^2 + 3J_2(T)\dot{\zeta}\ddot{\zeta} - J_3(T)\dot{\zeta}^3) \quad (\text{C.4})$$

## References

- [1] M. Ansorg and R. P. Macedo. Spectral decomposition of black-hole perturbations on hyperboloidal slices. *Phys. Rev. D*, 93(12):124016, 2016. arXiv: 1604.02261.
- [2] R. Archibald, K. Chen, A. Gelb, and R. Renaut. Improving tissue segmentation of human brain MRI through preprocessing by the Gegenbauer reconstruction method. *Neuroimage*, 20(1):489–502, 2003.
- [3] R. Archibald and A. Gelb. A method to reduce the Gibbs ringing artifact in MRI scans while keeping tissue boundary integrity. *IEEE Trans. Med. Imaging*, 21(4):305–19, 2002.
- [4] R. Archibald, J. Hu, A. Gelb, and G. Farin. Improving the Accuracy of Volumetric Segmentation Using Pre-Processing Boundary Detection and Image Reconstruction. *IEEE Trans. Image Process.*, 13(4):459–466, 2004.
- [5] L. Barack. Gravitational self-force in extreme mass-ratio inspirals. *Class. Quantum Gravity*, 26(21):213001, 2009.
- [6] L. Barack and L. M. Burko. Radiation reaction force on a particle plunging into a black hole. *Phys. Rev. D*, 62:084040, 2000.
- [7] L. Barack and C. O. Lousto. Computing the gravitational selfforce on a compact object plunging into a Schwarzschild black hole. *Phys. Rev. D*, 66:061502, 2002.
- [8] L. Barack and C. O. Lousto. Perturbations of Schwarzschild black holes in the Lorenz gauge: Formulation and numerical implementation. *Phys. Rev. D*, 72:104026, 2005.
- [9] Bengt Fornberg. *A Practical Guide to Pseudospectral Methods*. Cambridge University Press, 1998.
- [10] J. P. Boyd. *Chebyshev and Fourier Spectral Methods: Second Revised Edition (Dover Books on Mathematics)*. Dover Publications, 2001.
- [11] J. P. Boyd. Trouble with Gegenbauer reconstruction for defeating Gibbs’ phenomenon: Runge phenomenon in the diagonal limit of Gegenbauer polynomial approximations. *J. Comput. Phys.*, 204(1):253–264, 2005.
- [12] R. L. Brown. Some Characteristics of Implicit Multistep Multi-Derivative Integration Formulas. *SIAM Journal on Numerical Analysis*, 14(6):982–993, 1977.
- [13] R. L. Brown, Jr. *Multi-Derivative Numerical Methods for the Solution of Stiff Ordinary Differential Equations*. PhD Thesis, University of Illinois at Urbana-Champaign, Champaign, IL, USA, 1975.
- [14] J. C. Butcher, A. T. Hill, and T. J. T. Norton. Symmetric general linear methods. *BIT Numerical Mathematics*, 56(4):1189–1212, 2016.
- [15] P. Canizares and C. Sopena. Efficient pseudospectral method for the computation of the self-force on a charged particle: Circular geodesics around a Schwarzschild black hole. *Phys. Rev. D*, 79(8):084020, 2009.
- [16] P. Canizares and C. F. Sopena. Tuning time-domain pseudospectral computations of the self-force on a charged scalar particle. *Class. Quantum Gravity*, 28(13):134011, 2011.
- [17] P. Canizares, C. F. Sopena, and J. L. Jaramillo. Pseudospectral collocation methods for the computation of the self-force on a charged particle: Generic orbits around a Schwarzschild black hole. *Phys. Rev. D*, 82(4):044023, 2010.
- [18] C. Canuto, M. Hussaini, A. Quarteroni, and T. Zang. Spectral methods. 01 2006.
- [19] P. Chartier, E. Faou, and A. Murua. An Algebraic Approach to Invariant Preserving Integrators: The Case of Quadratic and Hamiltonian Invariants. *Numerische Mathematik*, 103:575–590, 2006.
- [20] K. S. Eckhoff. On discontinuous solutions of hyperbolic equations. *Comput. Methods Appl.*

- Mech. Engrg.*, 116(1-4):103–112, 1994.
- [21] K. S. Eckhoff. Accurate reconstructions of functions of finite regularity from truncated Fourier series expansions. *Math. Comp.*, 64(210):671–690, 1995.
  - [22] K. S. Eckhoff. On a high order numerical method for solving partial differential equations in complex geometries. *J. Sci. Comput.*, 12(2):119–138, 1997.
  - [23] K. S. Eckhoff. On a high order numerical method for functions with singularities. *Math. Comp.*, 67(223):1063–1087, 1998.
  - [24] K. S. Eckhoff and J. H. Rølfesnes. On nonsmooth solutions of linear hyperbolic systems. *J. Comput. Phys.*, 125(1):1–15, 1996.
  - [25] S. E. Field, J. S. Hesthaven, and S. R. Lau. Discontinuous Galerkin method for computing gravitational waveforms from extreme mass ratio binaries. *Class. Quantum Gravity*, 26(16):165010, 2009.
  - [26] S. E. Field, J. S. Hesthaven, and S. R. Lau. Persistent junk solutions in time-domain modeling of extreme mass ratio binaries. *Phys. Rev. D*, 81:124030, 2010.
  - [27] S. Gautam, A. Vañó Viñuales, D. Hilditch, and S. Bose. Summation by Parts and Truncation Error Matching on Hyperboloidal Slices. *Phys. Rev. D*, 103(8):084045, 2021.
  - [28] D. Gottlieb and S. Gottlieb. Spectral Methods for Discontinuous Problems. In *NA03 Dundee*, 2003.
  - [29] D. Gottlieb and C.-W. Shu. Resolution properties of the Fourier method for discontinuous waves. *Comput. Methods Appl. Mech. Eng.*, 116(1-4):27–37, 1994.
  - [30] D. Gottlieb and C.-W. Shu. On the Gibbs phenomenon IV. Recovering exponential accuracy in a subinterval from a Gegenbauer partial sum of a piecewise analytic function. *Math. Comput.*, 64(211):1081–1081, 1995.
  - [31] D. Gottlieb and C.-W. Shu. On the Gibbs phenomenon V: recovering exponential accuracy from collocation point values of a piecewise analytic function. *Numer. Math.*, 71(4):511–526, 1995.
  - [32] D. Gottlieb and C.-W. Shu. On the Gibbs Phenomenon III: Recovering Exponential Accuracy in a Sub-Interval From a Spectral Partial Sum of a Piecewise Analytic Function. *SIAM J. Numer. Anal.*, 33(1):280–290, 1996.
  - [33] D. Gottlieb and C.-W. Shu. On the Gibbs Phenomenon and Its Resolution. *SIAM Rev.*, 39(4):644–668, 1997.
  - [34] D. Gottlieb, C.-W. Shu, A. Solomonoff, and H. Vandeven. On the Gibbs phenomenon I: recovering exponential accuracy from the Fourier partial sum of a nonperiodic analytic function. *J. Comput. Appl. Math.*, 43(1):81–98, 1992.
  - [35] R. Haas. Scalar self-force on eccentric geodesics in Schwarzschild spacetime: A Time-domain computation. *Phys. Rev. D*, 75:124011, 2007.
  - [36] R. Haas. Time domain calculation of the electromagnetic self-force on eccentric geodesics in Schwarzschild spacetime. 12 2011.
  - [37] E. Hairer, C. Lubich, and G. Wanner. *Geometric Numerical Integration*. Number 31 in Springer Series in Computational Mathematics. Springer, Verlag Berlin Heidelberg, second edition edition, 2006.
  - [38] E. Harms, S. Bernuzzi, and B. Bruegmann. Numerical solution of the 2+1 Teukolsky equation on a hyperboloidal and horizon penetrating foliation of Kerr and application to late-time decays. 2013.
  - [39] E. Harms, S. Bernuzzi, A. Nagar, and A. Zenginoğlu. A new gravitational wave generation algorithm for particle perturbations of the kerr spacetime. *Classical and Quantum Gravity*, 31(24):245004, nov 2014.

- [40] A. Heffernan, A. C. Ottewill, N. Warburton, B. Wardell, and P. Diener. Accelerated motion and the self-force in Schwarzschild spacetime. *Class. Quant. Grav.*, 35(19):194001, 2018.
- [41] J. L. Jaramillo, R. P. Macedo, and L. A. Sheikh. Pseudospectrum and black hole quasi-normal mode (in)stability. *arXiv:2004.06434 [gr-qc, physics:hep-th, physics:math-ph]*, 2021. arXiv: 2004.06434.
- [42] J. L. Jaramillo, C. F. Sopuerta, and P. Canizares. Are time-domain self-force calculations contaminated by Jost solutions? *Phys. Rev. D*, 83(6):061503, 2011.
- [43] J.-H. Jung and B. D. Shizgal. Generalization of the inverse polynomial reconstruction method in the resolution of the Gibbs phenomenon. *J. Comput. Appl. Math.*, 172(1):131–151, 2004.
- [44] A. N. Krylov. *On approximate calculations, Lectures delivered in 1906*. Tipolitography of Birkenfeld, St. Petersburg, 1907.
- [45] C. Lanczos. *Discourse on Fourier series*. Oliver & Boyd, 1966.
- [46] Y. Lipman and D. Levin. Approximating piecewise-smooth functions. *IMA J. Numer. Anal.*, 30(4):1159–1183, 2009.
- [47] C. O. Lousto. Pragmatic approach to gravitational radiation reaction in binary black holes. *Phys. Rev. Lett.*, 84:5251–5254, 2000.
- [48] C. O. Lousto and R. H. Price. Understanding initial data for black hole collisions. *Phys. Rev. D*, 56:6439–6457, 1997.
- [49] C. Markakis, S. Bray, and A. Zenginoğlu. Symmetric integration of the 1+1 Teukolsky equation on hyperboloidal foliations of Kerr spacetimes. 3 2023.
- [50] C. Markakis, M. F. O’Boyle, P. D. Brubeck, and L. Barack. Discontinuous collocation methods and gravitational self-force applications. *Class. Quant. Grav.*, 38(7):075031, 2021.
- [51] C. M. Markakis, M. F. O’Boyle, D. Glennon, K. Tran, P. Brubeck, R. Haas, H.-Y. Schive, and K. Uryū. Time-symmetry, symplecticity and stability of euler-maclaurin and lanczos-dyche integration, 2019.
- [52] K. Martel and E. Poisson. A One parameter family of time symmetric initial data for the radial infall of a particle into a Schwarzschild black hole. *Phys. Rev. D*, 66:084001, 2002.
- [53] O. F. Næss and K. S. Eckhoff. A modified Fourier-Galerkin method for the Poisson and Helmholtz equations. In *J. Sci. Comput.*, volume 17, pages 529–539, 2002.
- [54] M. O’Boyle. *Time-symmetric integration of partial differential equations with applications to black hole physics*. Phd thesis, University of Illinois at Urbana-Champaign, Champaign, Illinois, May 2022. Available at <https://www.ideals.illinois.edu/items/125310>.
- [55] J. Piotrowska, J. M. Miller, and E. Schnetter. Spectral methods in the presence of discontinuities. *Journal of Computational Physics*, 390:527–547, 2019.
- [56] E. Poisson, A. Pound, and I. Vega. The Motion of Point Particles in Curved Spacetime. *Living Rev. Relativ.*, 14, 2011.
- [57] I. Rácz and G. Z. Tóth. Numerical investigation of the late-time Kerr tails. *Classical and Quantum Gravity*, 28(19):195003, 2011.
- [58] J. Sanz-Serna and M. Calvo. *Numerical Hamiltonian Problems*. Applied Mathematics and mathematical computation. Chapman & Hall, London, 1994.
- [59] C.-W. Shu and P. S. Wong. A note on the accuracy of spectral method applied to nonlinear conservation laws. *J. Sci. Comput.*, 10(3):357–369, 1995.
- [60] P. Sundararajan, G. Khanna, and S. Hughes. Towards adiabatic waveforms for inspiral into Kerr black holes: A new model of the source for the time domain perturbation equation. *Phys. Rev. D*, 76(10):104005, 2007.
- [61] P. Sundararajan, G. Khanna, S. Hughes, and S. Drasco. Towards adiabatic waveforms for inspiral into Kerr black holes. II. Dynamical sources and generic orbits. *Phys. Rev. D*,

- 78(2):024022, 2008.
- [62] A. Zenginoğlu. Hyperboloidal layers for hyperbolic equations on unbounded domains. *Journal of Computational Physics*, 230(6):2286–2302, 2011.
  - [63] A. Zenginoğlu, D. Núñez, and S. Husa. Gravitational perturbations of schwarzschild spacetime at null infinity and the hyperboloidal initial value problem. *Classical and Quantum Gravity*, 26(3):035009, 2009.
  - [64] A. i. e. i. f. Zenginoğlu. A geometric framework for black hole perturbations. *Phys. Rev. D*, 83:127502, 2011.
  - [65] A. Zenginoğlu. Hyperboloidal foliations and scri-fixing. *Classical and Quantum Gravity*, 25(14):145002, 2008.
  - [66] G. Zhong and J. E. Marsden. Lie-Poisson Hamilton-Jacobi theory and Lie-Poisson integrators. *Physics Letters A*, 133(3):134–139, 1988.